Orientational order in liquid crystals by combining ^{2}H and ^{13}C nuclear magnetic resonance spectroscopy and density functional theory calculations

Lucia Calucci,[1,*] Marco Geppi,[2] Alberto Marini,[2] and Carlo Alberto Veracini[2]
[1]*Istituto per i Processi Chimico-Fisici del CNR, via G. Moruzzi 1, 56124 Pisa, Italy*
[2]*Dipartimento di Chimica e Chimica Industriale, Università di Pisa, via Risorgimento 35, 56126 Pisa, Italy*
(Received 22 June 2010; published 7 October 2010)

Structural and orientational order properties of the liquid crystal 4,4′-bis-heptyl-azoxybenzene (**HAB**) have been obtained in its nematic and smectic-*A* phases by simultaneously analyzing several observables extracted from ^{2}H and ^{13}C nuclear magnetic resonance (NMR) spectra, i.e., ^{2}H quadrupolar, ^{2}H-^{1}H and ^{13}C-^{2}H dipolar couplings, as well as ^{13}C chemical shift anisotropy. ^{13}C experiments required the application of high-resolution solid-state NMR techniques like ^{1}H high-power decoupling and cross polarization, as well as the independent determination of chemical shift tensors by means of density functional theory (DFT) calculations, here performed taking into account the effect of the anisotropic medium by the polarizable continuum model method. The approach, consisting in the simultaneous analysis of all the ^{2}H and ^{13}C experimental data to derive orientational order parameters, and in the use of geometrical parameters determined by DFT methods, allows more detailed and reliable results to be obtained with respect to the traditional approach based on the sole analysis of ^{2}H experiments.

DOI: 10.1103/PhysRevE.82.041702 PACS number(s): 61.30.Gd, 82.56.−b, 76.60.−k, 71.15.Mb

I. INTRODUCTION

Nuclear magnetic resonance (NMR) spectroscopy is by now a well established method for investigating orientational order in thermotropic liquid crystalline phases [1–4]. To this aim several nuclei present (mainly ^{1}H and ^{13}C) or easily substituted (^{2}H) in the chemical structure of most liquid crystals have been investigated exploiting the different nuclear interactions. By virtue of its natural abundance and high concentration in liquid crystal molecules, ^{1}H has the advantage of a very high sensitivity; however, its spectra, which are determined by the homonuclear dipolar interaction, both intra- and intermolecular, show poor resolution and are often quite difficult to be interpreted. As a consequence, ^{1}H NMR spectroscopy is used to investigate orientational order only for small molecules in liquid crystalline solvents [5,6]. On the other hand, ^{2}H NMR spectra are quite simple and give site-specific information, being dominated by intra-molecular interactions, that is the quadrupolar interaction and the homonuclear ^{2}H-^{2}H and heteronuclear ^{2}H-^{1}H dipolar interactions. Therefore, deuterium is at present the most employed nucleus for studying orientational order in liquid crystalline phases. However, selectively deuterated samples, often costly and/or difficult to synthesize, are required. Moreover, the available deuterated positions in the liquid crystal molecules may not be sufficient to obtain quantitative reliable information on all molecular fragments. In this respect, ^{13}C presents many advantages, since, notwithstanding the low isotopic natural abundance, measurements can usually be performed on unlabeled samples, thus simultaneously determining chemical shift anisotropy (CSA) and, therefore, local order parameter values for all the carbon nuclei of the mesogen, provided a sufficient spectral resolution is obtained. Moreover, ^{2}H-^{13}C or ^{19}F-^{13}C dipolar couplings can also be obtained from ^{13}C spectra for liquid crystals containing a limited number of ^{2}H or ^{19}F nuclei [7–10]. Exploiting high-resolution solid-state NMR techniques, such as modern ^{1}H decoupling and ^{1}H-^{13}C cross-polarization (CP), at present a remarkable spectral resolution and signal-to-noise ratio can be achieved on liquid crystalline phases without undesirable heating of the sample also under static conditions [7]. ^{13}C NMR spectroscopy should therefore furnish the most complete set of data in terms of orientations for an accurate quantitative determination of molecular order parameters. Nevertheless, the interpretation of ^{13}C NMR spectra and the extraction of orientational parameters from the measured CSA values are not straightforward, requiring a separate determination of the molecular geometry and the principal components and location in the molecule of chemical shift tensors (CSTs). These data can now be obtained in good agreement with experimental CSTs [11] using computational methods rooted in the density functional theory (DFT) [12] with hybrid density functionals [13]. The effects of the anisotropic medium on both the molecular structure and CSTs can be effectively included in the calculations by means of the polarizable continuum model (PCM), recently implemented also for the calculation of nuclear magnetic shieldings and extended to anisotropic solvents, for which the dielectric tensor has to be defined instead of a simple dielectric constant [14,15].

In the present work, the orientational order of 4,4′-bis-heptyl-azoxybenzene (**HAB**, Fig. 1) in its nematic (N) and smectic-*A* (Sm*A*) liquid crystalline phases, previously studied by means of the sole ^{2}H NMR data [16], was reinvestigated also exploiting ^{13}C NMR data and DFT calculations. In particular ^{2}H NMR spectra were acquired on **HAB-d$_4$**, an isotopomer of **HAB** deuterated on positions 2 and 6 of both phenyl rings (Fig. 1), to obtain quadrupolar and ^{2}H-^{1}H dipolar splittings, whereas ^{13}C CP experiments under ^{1}H decoupling allowed well resolved ^{13}C spectra to be obtained for **HAB** and **HAB-d$_4$**, from which CSA values and

*Corresponding author; l.calucci@ipcf.cnr.it

 ©2010 The American Physical Society

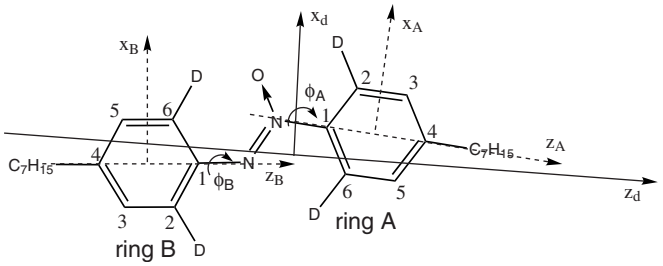

FIG. 1. Molecular structure and labeling of atoms of **HAB** and **HAB-d$_4$** and axis systems used in the orientational order analysis.

^{13}C-^{2}H dipolar couplings for the aromatic carbons were determined. The obtained ^{2}H and ^{13}C data were simultaneously analyzed to give orientational order parameters for the aromatic core by means of a global fitting procedure using optimized geometrical parameters and ^{13}C CSTs computed at the DFT/PCM level. This approach, combining state of the art techniques for both solid state NMR and DFT, allowed more reliable orientational order parameters to be determined.

II. EXPERIMENTAL

A. Materials

HAB and its isotopomer **HAB-d$_4$** (isotopic enrichment 98%, as determined by ^{1}H NMR in solution) were prepared as reported in Ref. [16]. The sequence of phases and phase transition temperatures, determined by polarized optical microscopy and DSC measurements, was Cr—307.1 K—Sm*A*—327.4 K—N—344.1 K—I and Cr—306.9 K—Sm*A*—326.9 K—N-343.8 K—I for **HAB** and **HAB-d$_4$**, respectively.

B. NMR experiments

^{1}H and ^{13}C NMR spectra in solution were recorded at 298 K on a Bruker AMX300 spectrometer, operating at 300.13 MHz for ^{1}H and at 75.47 MHz for ^{13}C, equipped with a 5 mm probehead. Tetramethylsilane (TMS) was used as reference internal standard for chemical shift.

^{2}H NMR experiments within the mesophases of **HAB-d$_4$** were carried out on a Bruker AMX300 spectrometer operating at the deuterium frequency of 46.04 MHz, equipped with a 5 mm probehead. The spectra were acquired by using the quadrupolar echo pulse sequence with a 90° pulse of 9.5 μs, a time interval between two 90° pulses of 35 μs, a recycle delay of 3 s, and 200 scans.

Static ^{13}C direct excitation (DE) and cross-polarization (CP) NMR experiments on **HAB** and **HAB-d$_4$** were carried out on a double-channel Varian Infinity Plus 400 spectrometer, working at 100.56 MHz for ^{13}C, equipped with a 5 mm goniometric probe. High-power ^{1}H decoupling was realized using the SPINAL 64 scheme [17]. The ^{1}H 90° pulse length was 4.2 μs, the recycle delay was 20 s, and the contact time was 5.0 ms and 7.0 ms for **HAB** and **HAB-d$_4$**, respectively. 16–32 scans were acquired depending on the sample. The chemical shift scale was referred to the signal of TMS using hexamethylbenzene as an external reference.

^{2}H and ^{13}C experiments in the mesophases were performed on samples macroscopically aligned within the magnet by slow cooling from the isotropic to the N phase. Spectra were recorded on cooling waiting at least 15 min for temperature equilibration; the temperature was always controlled within ± 0.2 K.

TABLE I. Selection of geometrical parameters determined from DFT calculations *in vacuo* and in the liquid crystalline medium.

Ring A		Ring B	
Bond lengths and distances *in vacuo* (Å)			
C3H2	2.167	C3H2	2.150
C5H6	2.162	C5H6	2.155
H2H3	2.492	H2H3	2.459
H5H6	2.484	H5H6	2.479
Bond lengths and distances in medium (Å)			
C3H2	2.164	C3H2	2.148
C5H6	2.160	C5H6	2.155
H2H3	2.486	H2H3	2.455
H5H6	2.479	H5H6	2.478
Angles *in vacuo* (°)			
H2C2C3	121.7	H2C2C3	120.4
H6C6C5	121.4	H6C6C5	120.9
H2C3C2	25.1	H2C3C2	25.6
H6C5C6	25.3	H6C5C6	25.6
Angles in medium (°)			
H2C2C3	121.3	H2C2C3	120.1
H6C6C5	121.1	H6C6C5	120.7
H2C3C2	25.3	H2C3C2	25.8
H6C5C6	25.4	H6C5C6	25.7

C. Calculations of optimized molecular geometries and chemical shift tensors

The molecular structures of **HAB** and **MAB** (4,4′-bis-methyl-azoxybenzene) were built using GaussView 4.1 (Gaussian, Inc., Wallingford, CT) and all of the calculations were performed with the development version E.05 of the *Gaussian 03* package [18]. The geometries were optimized using DFT methods with the B3LYP/6–31G(d) combination of hybrid functional and basis set [19–21], both *in vacuo* and simulating the solvent effect using the integral equation formalism of the polarizable continuum model (IEF-PCM) [15]; in the latter case, the experimental isotropic dielectric permittivity (ε^{iso}) values of 3.35 and 3.49 [22] were used in the calculations of **HAB** at 233 K (N phase) and 311 K (Sm*A* phase), respectively. PCM cavities were con-

TABLE II. Chemical shift tensor principal components (δ_{xx}, δ_{yy}, δ_{zz}, in ppm) determined from DFT calculations and angles (γ, in degrees) between the z axis of the chemical shift tensor principal axis system and the ring para axis.

	Ring A					Ring B			
Cn	δ_{xx}	δ_{yy}	δ_{zz}	γ	Cn	δ_{xx}	δ_{yy}	δ_{zz}	γ
				In vacuo					
1	145.4	69.6	226.7	180.3	1	164.1	35.9	229.9	4.6
2	149.9	0.2	219.5	−116.0	2	152.9	9.4	209.7	−66.1
3	135.8	17.9	229.9	−59.5	3	132.8	19.4	232.4	−120.7
4	190.8	8.9	245.0	0.9	4	191.6	8.4	240.8	180.0
5	134.3	18.9	228.5	59.6	5	131.4	18.7	232.6	118.5
6	147.6	5.0	214.3	115.2	6	144.6	21.5	226.7	66.0
				N phase					
1	144.8	70.0	225.0	180.2	1	163.4	36.1	229.4	4.7
2	149.9	0.2	219.3	−115.5	2	151.7	9.6	209.1	−66.9
3	139.1	16.7	231.2	−59.4	3	135.2	18.2	232.6	−120.8
4	195.3	8.9	246.1	1.1	4	196.1	8.3	242.8	181.0
5	135.8	17.7	229.1	59.7	5	134.5	17.5	233.6	118.5
6	146.5	4.6	213.8	115.7	6	146.1	20.8	227.3	66.3
				Sm*A* phase					
1	145.2	70.0	225.1	180.3	1	163.2	36.1	229.5	4.6
2	150.0	0.2	219.4	−115.4	2	151.8	9.9	209.1	−66.3
3	139.2	16.7	231.2	−59.7	3	135.0	18.3	232.9	−120.8
4	195.3	8.8	246.6	0.8	4	196.1	8.3	242.8	180.5
5	135.8	17.9	229.0	59.4	5	134.4	17.6	233.7	118.5
6	146.6	4.7	214.0	115.5	6	146.2	20.8	227.3	66.5

structed from radii obtained by applying the United Atom Topological Model to the atomic radii of the UFF force field [23] as implemented in the GAUSSIAN 03 code.

In the conformational analysis of **MAB** *in vacuo*, a complete Potential Energy Surface (PES) was obtained by scanning the ϕ_A and ϕ_B dihedral angles in steps of 15°; the conformers geometry was optimized without constraints but the dihedral angles in order to obtain fully relaxed structures.

^{13}C nuclear shielding tensors were calculated for all aromatic carbons of **HAB** and **MAB** at the DFT level of theory using the method of Gauge-Including Atomic Orbitals (GIAO) [24] by a combination [MPW1PW91/6-311 +G(d,p)] of hybrid functional and basis set [25–27]. Calculations were performed *in vacuo* and in the anisotropic environment ("in medium") using the IEF-PCM method [15]; in the latter case, the geometries optimized in the N and Sm*A* phases were used in combination with the experimental components of the dielectric permittivity tensor [22], $\varepsilon_{\parallel}$ and $\varepsilon_{\perp}$, at 233 K ($\varepsilon_{\parallel}$=3.49, $\varepsilon_{\perp}$=3.28) and 311 K ($\varepsilon_{\parallel}$=3.36, $\varepsilon_{\perp}$=3.55), respectively. ^{13}C chemical shift tensors were obtained by referring the absolute chemical shielding tensors to the absolute shielding of TMS (185.97 ppm), calculated at the same level of theory.

D. Data analysis

A nonlinear least-squares fitting procedure was applied to the set of ^{2}H quadrupolar splittings, ^{13}C chemical shift anisotropies, and ^{2}H-^{1}H and ^{13}C-^{2}H dipolar splittings, measured at all investigated temperatures, to determine orientational order parameters using a software purposely written in Mathematica (Wolfram Research Inc.) language.

III. RESULTS AND DISCUSSION

A. Geometry optimization and chemical shift tensor calculations

Geometry optimization and ^{13}C chemical shift tensor (CST) calculations for **HAB** were performed at the DFT level of theory both *in vacuo* and by considering the effect of the medium through the PCM model [14,15]. In both cases, in the minimum energy conformation the **HAB** core had the two phenyl rings and the azoxy group coplanar, in agreement to what reported for azoxy-benzene [28] and 4,4′-dibuthyl-azoxybenzene [29], while the aliphatic chains showed an *all trans* conformation. Indeed, the core planar geometry allows the interaction between the π electrons of the aromatic rings and the azoxy linking group. The angle between the para axes of the two phenyl rings was found to be equal to 11.9° and 11.6° in the *in vacuo* and in medium (for both N and Sm*A* phases) geometry optimizations, respectively. Moreover, small differences were found for all molecular geometry parameters by considering or not the medium effect in the calculations (Table I), whereas negligible differences were found between geometries optimized

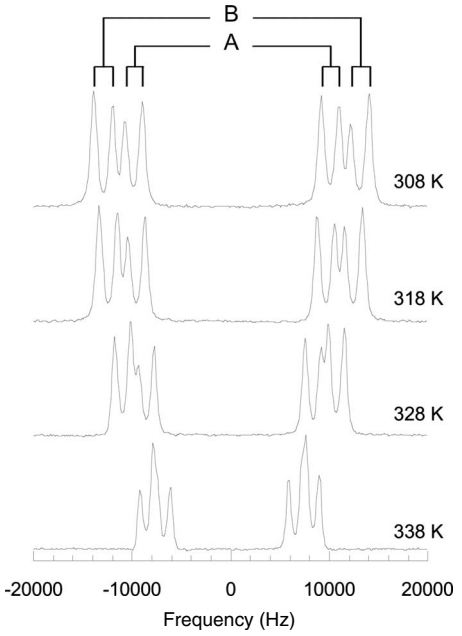

FIG. 2. Selection of ^{2}H NMR spectra of **HAB-d$_4$**.

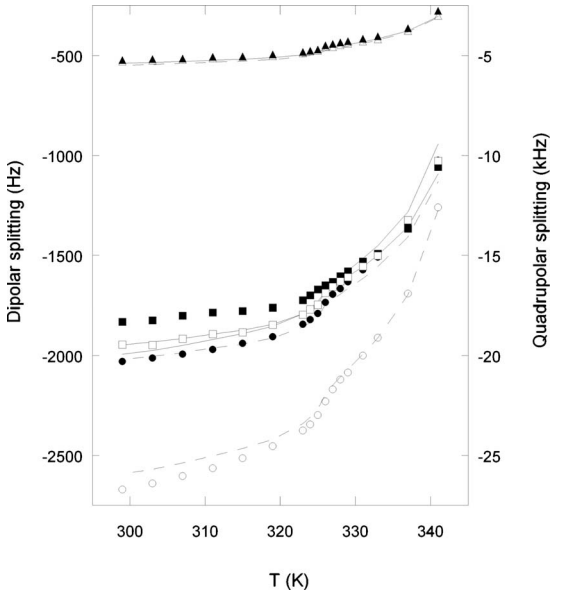

FIG. 3. Experimental (symbols) and calculated (lines) ^{2}H-^{1}H (squares) and ^{13}C-^{2}H (triangles) dipolar splittings and ^{2}H quadrupolar splittings (circles) of **HAB-d$_4$** as a function of temperature. Full and empty symbols and solid and dashed lines refer to deuteria on ring A and B, respectively.

in the N and Sm*A* phases. On the other hand, it must be pointed out that the bond lengths and angles determined for the aromatic rings differed significantly from the "regular" geometrical parameters usually employed in orientational order studies by means of dipolar and quadrupolar couplings analysis, i.e., CCH(D) angles of 120° and C-H(D) and C-C bond lengths of 1.09 and 1.40 Å, respectively, implying distances between hydrogens in ortho positions of 2.49 Å. In particular, distorsions of the phenyl ring geometry gave CCH(D) bond angles in positions 2 and 6 significantly different from 120° for both rings and distances between hydrogens in ortho positions significantly shorter than 2.49 Å for ring B.

As far as CSTs are concerned, small but detectable differences were found between calculations performed *in vacuo* and in the anisotropic medium, whereas almost identical CSTs were obtained by the PCM method using dielectric permittivity tensor values measured in the N and Sm*A* phase (Table II).

In order to justify the use of the sole minimum energy planar conformation and the corresponding ^{13}C CSTs in the orientational order study, a conformational analysis of the aromatic core was performed *in vacuo* on the model compound 4,4′-dimethyl-azoxybenzene (**MAB**). This approach, allowing the computational time to be considerably reduced, is justified on the basis of preliminary tests on the effects of alkyl chain length on core conformations as well as of results reported in the literature for other calamitic mesogens [28,30]. The analysis was carried out by scanning the ϕ_A and ϕ_B dihedral angles (Fig. 1); as found for **HAB**, the obtained potential energy surface (PES) has a minimum at $\phi_A = \phi_B = 0°$, corresponding to the situation where the phenyl rings and the azoxy group are coplanar. Moreover, the two lowest energy profiles obtained scanning one of the angles by keeping the other equal to 0°, that is maintaining the π-π interaction between one ring and the azoxy group, indicated that a lower torsional barrier and bigger geometry changes, in particular of the angle between the para axes of the rings, are associated to the rotation of ring B (see Supplementary Material [31]), probably due to the interaction between the azoxy oxygen and the hydrogen in position 2 of ring B. However, the molecular structure is not significantly affected by rotations of the phenyl rings by angles corresponding to the most populated conformations (ϕ_A and ϕ_B within $\pm 15°$); this is reflected on the fact that bond lengths and angles obtained by a Boltzmann average over all the conformations differ from those obtained for the minimum energy conformation only to the fourth and second digit, respectively. Similar results were obtained for CSTs; in fact, although a dependence of CST values on conformation was found (see Supplementary Material [31]), in the most populated states the CSTs were practically identical, so that there was a substantial coincidence between the Boltzmann-averaged CSTs and those calculated for the minimum energy conformation (see Supplementary Material [31]).

B. ^{2}H and ^{13}C NMR spectra

^{2}H NMR spectra were recorded on **HAB-d$_4$**, deuterated on positions 2 and 6 of both phenyl rings, at different temperatures throughout the N and Sm*A* phases; representative spectra are reported in Fig. 2. Each pair of deuteria of the same aromatic ring, made equivalent by fast 180° ring flips about the para axis, gave a quadrupolar doublet further split by dipolar coupling of deuteria with protons in ortho position. Therefore, at each temperature, absolute values of two dipolar and two quadrupolar splittings could be determined from the spectrum; these values regularly increased by decreasing the temperature within each mesophase and showed

TABLE III. ^{13}C isotropic chemical shift values (ppm) determined for **HAB** by GIAO-DFT calculations *in vacuo* (δ_V^{GIAO}), and in the N (δ_N^{GIAO}) and Sm*A* (δ_{SmA}^{GIAO}) phases, and by NMR experiments in $CDCl_3$ solution (δ_{CDCl_3}) and in the melt phase (δ_{Melt}); ^{13}C isotropic chemical shift values (ppm) measured for **HAB-d$_4$** by NMR experiments in $CDCl_3$ solution (δ_{CDCl_3}).

	HAB					HAB-**d$_4$**
Cn	δ_V^{GIAO}	δ_N^{GIAO}	δ_{SmA}^{GIAO}	δ_{Melt}	δ_{CDCl_3}	δ_{CDCl_3}
1A	147.2	146.6	146.8	146.4	146.3	146.1
2A	123.2	123.1	123.2	122.3	122.1	121.8
3A	127.9	129.0	129.0	128.3	128.5	128.4
4A	148.3	150.1	150.2	146.7	146.7	146.7
5A	127.2	127.5	127.6	128.3	128.5	128.4
6A	122.3	121.6	121.8	122.3	122.1	121.8
1B	143.3	143.0	142.9	142.6	142.0	141.7
2B	124.0	123.5	123.6	126.1	125.6	125.3
3B	128.2	128.7	128.7	128.3	128.5	128.4
4B	146.9	149.0	149.1	144.4	144.9	144.9
5B	127.6	128.5	128.6	128.3	128.5	128.4
6B	130.9	131.4	131.4	126.1	125.6	125.3

a discontinuity at the N-Sm*A* phase transition (Fig. 3). In a previous study performed on **HAB-d$_{12}$**, deuterated on positions 2, 3, 5, and 6 of both aromatic rings and on the first methylene group of both chains [16], the largest quadrupolar and the corresponding largest dipolar splittings were attributed to ring A, that is to the ring bonded to the NO group on the basis of the comparison of **HAB-d$_{12}$** and **HB-d$_{12}$** (4,4′-bis-heptyl-azobenzene deuterated on the same positions as **HAB-d$_{12}$**) spectra. This assignment will be discussed in the following taking into account the optimized geometrical parameters determined by DFT calculations.

^{13}C NMR spectra were recorded under ^1H decoupling on both **HAB** and **HAB-d$_4$** in the isotropic melt phase and in $CDCl_3$ solution. Eight singlets, corresponding to the chemically nonequivalent aromatic carbons, were detected in the aromatic region for **HAB**; on the other hand, the aromatic spectral region of **HAB-d$_4$** showed six singlets and two triplets, the last arising from the ^{13}C-^2H scalar coupling between carbons in position 2 and 6 of both phenyl rings and the directly bonded deuteria. As it can be observed, a low-frequency shift was found for all aromatic carbons due to the deuterium isotope effect on ^{13}C nuclear shielding [32–34]. By considering the dependence of this isotopic effect on the number of bonds between carbons and deuteria, the results of selective ^1H-^{13}C HMQC spectra of **HAB** in $CDCl_3$, as well as the isotropic chemical shift values resulting from DFT calculations, the ^{13}C NMR spectra of **HAB** aromatic carbons were assigned as reported in Table III. The chemical shifts measured in $CDCl_3$ solution and in the melt isotropic phase were very similar and in good agreement with those calculated by the GIAO-DFT method.

^{13}C CP NMR spectra under proton decoupling were recorded at different temperatures in the mesophases of both **HAB** and **HAB-d$_4$** uniformly aligned with the director parallel to the magnetic field; expansions of the aromatic regions of representative spectra are shown in Fig. 4. In the case of **HAB** up to eight peaks were observed for aromatic carbons, depending on the temperature, all showing high-frequency shifts with respect to the corresponding isotropic signals due to the anisotropic components of the chemical shift (δ^{aniso}). Indeed, each pair of carbons C2-C6, and C3-C5 on each phenyl ring, made equivalent by fast ring flip, gave a peak in the 140–160 ppm spectral region; two narrow peaks ascribable to quaternary carbons in position 4 of each ring were present in the 190–225 ppm spectral region, whereas quaternary carbons in position 1 of both rings gave undistinguishable broad signals in the 180–215 ppm spectral region. The line broadening of the last peaks could be ascribed to coupling of ^{13}C nuclei in position 1 to directly bonded ^{14}N nuclei [35]. Moreover, two narrower and two broader peaks were observed for protonated carbons; on the basis of broadening due to ^{13}C-^{14}N dipolar coupling the broader peaks could be ascribed to carbons C2 and C6. The

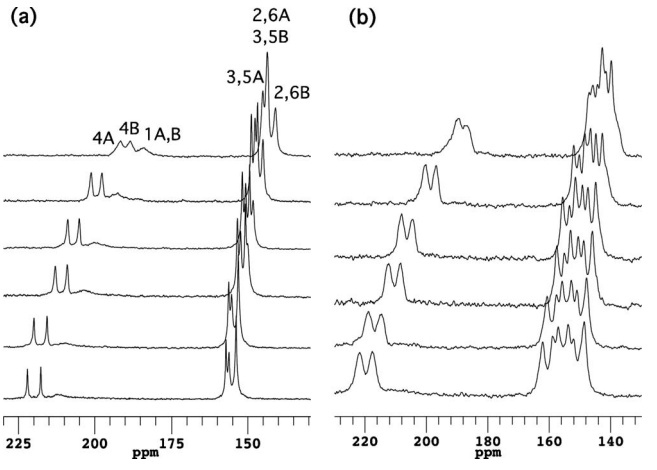

FIG. 4. ^{13}C CP NMR spectra of (a) **HAB** and (b) **HAB-d$_4$** recorded under proton decoupling at, from top to bottom, 341, 337, 331, 327, 321, and 311 K.

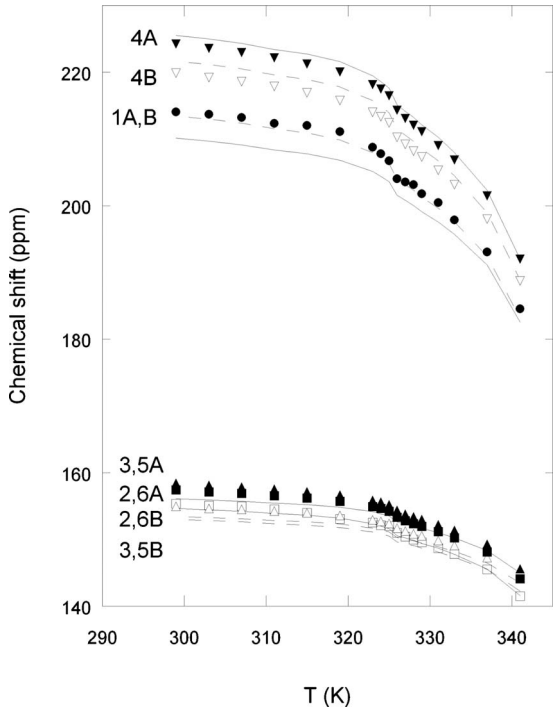

FIG. 5. Experimental (symbols) and calculated (lines) ^{13}C chemical shifts of carbons in position 1 (circles), 2,6 (squares), 3,5 (up triangles), and 4 (down triangles) of the aromatic rings of **HAB** as a function of temperature. Full and empty symbols and solid and dashed lines refer to deuteria on ring A and B, respectively.

chemical shift values of all carbons increased by decreasing the temperature within the mesophases, as expected for aromatic carbons in calamitic phases, and showed a discontinuity at the N-S_A phase transition (Fig. 5). the values of the chemical shift anisotropies (δ^{aniso}) were obtained at each temperature by subtracting the isotropic value measured in the isotropic phase (δ^{iso}) from the chemical shift value measured in the mesophase (δ^{obs}),

$$\delta^{obs} = \delta^{iso} + \delta^{aniso}. \tag{1}$$

The ^{13}C CP NMR spectra of **HAB-d$_4$** were similar to those of **HAB** in the 180–225 ppm region, the only difference being the further broadening of C1 signals due to ^{13}C-^{2}H coupling, which rendered these signals undetectable at some temperatures. On the other hand, in the 140–170 ppm range **HAB-d$_4$** gave much more complex signals than **HAB** because of the ^{13}C-^{2}H couplings, the deuterium isotope effect on ^{13}C chemical shift, and the different ^{1}H-^{13}C CP efficiency of protonated and deuterated carbons. In particular, a spectral analysis showed that this spectral region is dominated by the signals of C3 and C5 of both phenyl rings which, being protonated, give efficient CP and very small isotope shift and are split in three lines due to dipolar coupling with deuteria in position 2 and 6. On the contrary, deuterated C2 and C6 carbons are substantially undetectable given the expected poor CP efficiency and the split in three lines by the ^{13}C-^{2}H coupling. On the basis of the features of both **HAB** and **HAB-d$_4$** ^{13}C spectra, signals could be unambiguously assigned to C2 and C6 and to C3 and C5 carbons but no sound attribution to one or the other of the rings could be made. The ^{13}C-^{2}H splittings (Δ_{ij}), that is the separation between the three lines due to coupling between the ^{13}C nucleus i in position 3 or 5 and the ^{2}H nucleus j in position 2 or 6, respectively, were determined from the spectra of **HAB-d$_4$** at each investigated temperature; the splitting absolute values increased on cooling within each mesophase as shown in Fig. 3.

C. Determination of orientational order parameters

Orientational order parameters of the aromatic core of **HAB** were determined from the quite large set of NMR data available, that is ^{2}H quadrupolar splittings, ^{1}H-^{2}H and ^{13}C-^{2}H dipolar couplings, and ^{13}C chemical shift anisotropies obtained from ^{2}H and ^{13}C NMR spectra of **HAB** and **HAB-d$_4$** at different temperatures, using a nonlinear least-squares fitting procedure. In particular, all the data were analyzed together by means of a global fitting procedure to obtain order parameters for the whole core in its most likely conformation, whereas several data subsets were separately analyzed in order to discriminate among different possible signal assignments. On the basis of the $D_{\infty h}$ symmetry of the N and Sm*A* phases, two independent order parameters, S^d_{zz} and $S^d_{xx}-S^d_{yy}$, with (x_d, y_d, z_d) being the principal axis system where the Saupe matrix is diagonal, describe the order of the **HAB** aromatic core, which is here considered planar and rigid except for the 180° flip of the rings. Two independent parameters are also sufficient to describe the local orientational order of each phenyl ring with the z axis coincident with the ring para axis (Fig. 1).

Quadrupolar splittings of deuterium i ($\Delta\nu_i$) are related to the local order parameter relative to the C-^{2}H bond (S^i_{CD}) by Eq. (2),

$$\Delta\nu_i = \frac{3}{2} q S^i_{CD}, \tag{2}$$

where q is the quadrupolar coupling constant, here assumed equal to 185 000 Hz. ^{2}H-^{1}H and ^{13}C-^{2}H splittings (Δ_{ij}), for which the only contribution of direct dipolar coupling is considered, can be expressed in terms of the order parameter S_{ij} relative to the internuclear i-j direction and the equilibrium internuclear distance r_{ij} as

$$\Delta_{ij} = -2\frac{\gamma_i \gamma_j h S_{ij}}{4\pi^2 r^3_{ij}}. \tag{3}$$

For each ^{13}C nucleus i the chemical shift anisotropy is related to the elements S_{ab} of the Saupe ordering matrix defined in the phenyl ring frame and to chemical shift tensor elements ($\delta_{i,ab}$) written in the same frame by Eq. (4),

$$\delta^{aniso}_i = \frac{2}{3}\left[\Delta\delta_i S_{zz} + \frac{1}{2}(\delta_{i,xx} - \delta_{i,yy})(S_{xx} - S_{yy})\right], \tag{4}$$

where

$$\Delta\delta_i = \delta_{i,zz} - \frac{1}{2}(\delta_{i,xx} + \delta_{i,yy}). \tag{5}$$

The chemical shift tensor elements in the phenyl ring frame can be obtained from those in the principal frame by a rotation by γ (Table II) in the ring plane.

The local order parameters can, in turn, be expressed in terms of the elements of the Saupe order matrix relative to a frame fixed on a rigid molecular fragment using the relationship

$$S_{\alpha\beta} = \sum_{i,j} l_{\alpha i} S_{ij} l_{j\beta}, \tag{6}$$

where $l_{\alpha i}$ is the direction cosine between the α and the i axes.

In the analysis, the above equations were employed to relate experimental quadrupolar, dipolar and chemical shift data to order parameters using geometrical parameters (bond lengths and angles) and CSTs determined by DFT calculations using the PCM model (Tables I and II). On the basis of the molecular geometry and considering that **HAB** aligns with the director parallel to the external magnetic field and the principal order axis is expected to lie close to the long molecular axis, all dipolar and quadrupolar splittings were considered negative. On the other hand, all the δ^{aniso} values were positive. The angle between the ring para axes was fixed to the value of 11.6° as determined by geometry optimization in medium.

When quadrupolar and dipolar splittings were used to obtain orientational order parameters for the single aromatic rings an excellent reproduction of experimental data was obtained if the set of bigger splittings was attributed to either ring A or B. In fact, in both cases ^{13}C-^{2}H dipolar couplings, ^{2}H-^{1}H dipolar couplings and ^{2}H quadrupolar couplings were reproduced with errors lower than 10, 40, and 20 Hz, respectively. As expected, the values of the principal order parameter S_{zz} were higher for the ring with bigger splittings, whereas biaxiality values were very small (lower than 0.04 in absolute value) for both rings.

A very good reproduction of experimental data was also obtained when all the dipolar and quadrupolar splittings were fitted to give orientational order parameters for the whole aromatic core assigning the bigger splittings either to ring A or B, even though in the second case the experimental data reproduction was slightly better (see Supplementary Material [31]), giving maximum deviations between experimental and calculated data of about 10, 40, and 400 Hz for ^{13}C-^{2}H, ^{1}H-^{2}H dipolar splittings, and ^{2}H quadrupolar splittings, respectively. It must be pointed out that when the bigger splittings are assigned to ring A the principal order axis z_d of the aromatic core forms angles of 2.4° and 14.0° with the para axes of rings A and B, respectively; in the other case, z_d lies in between the para axes of rings A and B, forming angles of 7.4° and −4.2° with them, respectively.

Also δ^{aniso} values were employed in single ring fittings in order to choose the best attribution of data to ring A or B. To this aim different assignments of ^{13}C signals were tested within the constraints above discussed. These tests, however, only allowed the assignment of the signal with the highest chemical shift at all temperatures to C4 of ring A. The maximum deviations between experimental and calculated ^{13}C δ^{aniso} was of about 3.3 ppm.

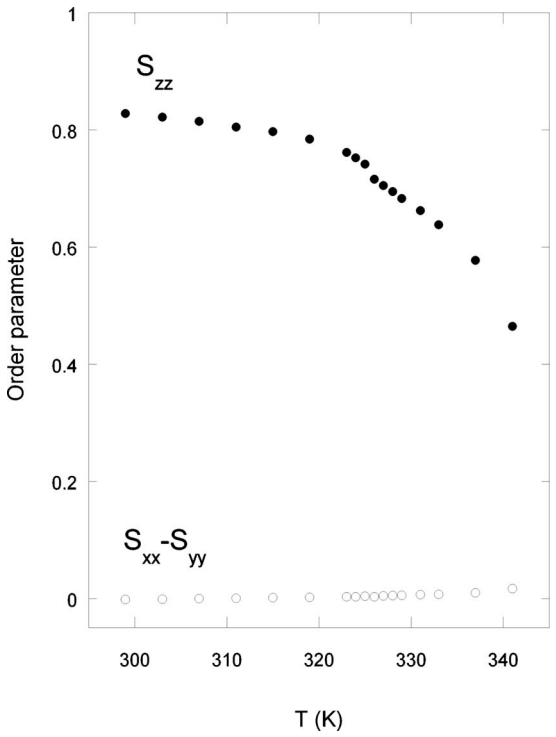

FIG. 6. Best fit principal order parameter S^d_{zz} (full circles) and biaxiality $S^d_{xx}-S^d_{yy}$ (empty circles) values of **HAB** as a function of temperature.

Taking into account all these findings, four different sets of ^{13}C and ^{2}H signal assignments could still be possible and were all used in a global fitting analysis where all the data for both rings were simultaneously considered to obtain the orientational order parameters of the aromatic core and the location of the principal order frame. On the basis of this analysis, the best results were found with the assignment reported in Figs. 2–5, corresponding to the orientational order parameters reported in Fig. 6 and to angles between z_d and the para axes of rings A and B of 7.2° and −4.4°, respectively. As shown in Figs. 3 and 5, the reproduction of the experimental data is quite good, with maximum deviations of about 20, 110, 750 Hz, and 4 ppm for ^{13}C-^{2}H, ^{1}H-^{2}H dipolar splittings, ^{2}H quadrupolar splittings, and ^{13}C δ^{aniso}, respectively. It must be noticed that the order parameters S_{zz} here obtained, although showing the same trend with temperature, are 10–15 % larger than those previously obtained from ^{2}H data only, when a regular geometry, a null biaxiality of the aromatic core, and the alignment of the principal axis order with the para axis of the A ring were assumed [16].

IV. SUMMARY

The orientational order of HAB, previously studied by ^{2}H NMR spectroscopy [16], was revisited by applying a multinuclear approach where ^{2}H spectral parameters (^{2}H quadrupolar and ^{2}H-^{1}H dipolar couplings) are combined and simultaneously analyzed in a global fitting with ^{13}C spectral parameters (^{13}C chemical shift anisotropies and ^{13}C-^{2}H dipolar couplings), obtained using up-to-date solid state NMR

techniques. The analysis of ^{13}C chemical shift anisotropies required the use of DFT methods to calculate the shielding tensors. Moreover, DFT methods were used for the calculation of geometrical parameters, rather than using a "standard" molecular geometry, as usually done. The DFT calculations performed are based on the IEF-PCM method to take into account the effects of the liquid crystalline medium. The approach here proposed and applied allowed a substantial increase of the reliability of the results obtained with respect to the traditional studies based on ^{2}H NMR data only. This was due on one side to the improvement of the quality of the geometrical parameters used and on the other side to the simultaneous analysis of a large and variegated set of experimental data. The latter acts by reducing the biasing effects of potential systematic errors (for instance arising from the assumption of quadrupolar coupling constants, of a given geometry, etc.) and, moreover, by increasing the robustness of the fitting procedure. This approach appears of general applicability to all the cases when selectively deuterated mesogens are available.

ACKNOWLEDGMENTS

Professor B. Mennucci is acknowledged for her support in DFT calculations.

[1] *Nuclear Magnetic Resonance of Liquid Crystals*, edited by J. W. Emsley (Reidel Publishing Company, Dordrecht, Germany, 1985).
[2] R. Y. Dong, *Nuclear Magnetic Resonance of Liquid Crystals* (Springer-Verlag, New York, 1994).
[3] L. Calucci and C. A. Veracini, in *Encyclopedia of Spectroscopy and Spectrometry*, edited by J. C. Lindon, G. E. Tranter, and J. L. Holmes (Academic, San Diego, 2000), Vol. 2, pp. 1179–1186.
[4] R. Y. Dong, Annu. Rep. NMR Spectrosc. **53**, 67 (2004).
[5] G. Celebre, F. Castiglione, M. Longeri, and J. W. Emsley, J. Magn. Reson., Ser. A **121**, 139 (1996).
[6] *NMR of Ordered Liquids*, edited by E. E. Burnell and C. A. de Lange (Kluwer Academic, Dordrecht, 2003).
[7] B. M. Fung, Prog. Nucl. Magn. Reson. Spectrosc. **41**, 171 (2002).
[8] D. Catalano, M. Geppi, A. Marini, C. A. Veracini, S. Urban, J. Csub, W. Kuczynski, and R. Dabrowski, J. Phys. Chem. C **111**, 5286 (2007).
[9] M. Geppi, A. Marini, C. A. Veracini, S. Urban, J. Csub, W. Kuczynski, and R. Dabrowski, J. Phys. Chem. B **112**, 9663 (2008).
[10] S. Borsacchi, L. Calucci, J. Csub, R. Dabrowski, M. Geppi, W. Kuczynski, A. Marini, B. Mennuci, and S. Urban, J. Phys. Chem. B **113**, 15783 (2009).
[11] R. Y. Dong, M. Geppi, A. Marini, V. Hamplova, M. Kaspar, C. A. Veracini, and J. Zhang, J. Phys. Chem. B **111**, 9787 (2007).
[12] R. G. Parr and W. Yang, *Density-Functional Theory of Atoms and Molecules* (Oxford University Press, New York, 1989).
[13] *Calculation of NMR and EPR Parameters*, edited by M. Kaupp, V. G. Malkin, and M. Bühl (Wiley-VHC, Würzburg, 2004).
[14] J. Tomasi, in *Continuum Solvation Models in Chemical Physics: Theory and Applications*, edited by B. Mennucci and R. Cammi (John Wiley and Sons, Ltd., Chichester, UK, 2007), Chap. 1.
[15] E. Cancès, B. Mennucci, and J. Tomasi, J. Chem. Phys. **107**, 3032 (1997).
[16] D. Catalano, C. Forte, C. A. Veracini, J. W. Emsley, and G. N. Shilstone, Liq. Cryst. **2**, 345 (1987).
[17] B. M. Fung, A. K. Khitrin, and K. Ermolaev, J. Magn. Reson. **142**, 97 (2000).
[18] M. J. Frisch *et al.*, Gaussian, Inc., Wallingford, CT, 2006.
[19] A. D. Becke, Phys. Rev. A **38**, 3098 (1988).
[20] C. Lee, W. Yang, and R. G. Parr, Phys. Rev. B **37**, 785 (1988).
[21] P. J. Stephens, F. J. Devlin, C. H. Chabalowski, and M. Frisch, J. Phys. Chem. **98**, 11623 (1994).
[22] W. H. de Jeu, Th. W. Lathouwers, and P. Bordewijk, Phys. Rev. Lett. **32**, 40 (1974).
[23] C. J. Casewit, K. S. Colwell, and A. K. Rappe, J. Am. Chem. Soc. **114**, 10046 (1992).
[24] R. Ditchfield, Mol. Phys. **27**, 789 (1974).
[25] J. P. Perdew, in *Electronic Structure of Solids '91*, edited by P. Ziesche and H. Eschig (Akademie Verlag, Berlin, 1991).
[26] C. Adamo and V. Barone, J. Chem. Phys. **108**, 664 (1998).
[27] B. J. Lynch, Y. Zhao, and D. G. Truhlar, J. Phys. Chem. A **107**, 1384 (2003).
[28] T. Tsuji, H. Takashima, H. Takeuchi, T. Egawa, and S. Konaka, J. Mol. Struct. **554**, 203 (2000).
[29] I. Cacelli, A. Cimoli, L. De Gaetani, G. Prampolini, and A. Tani, J. Chem. Theory Comput. **5**, 1865 (2009).
[30] K. Inoue, H. Takeuchi, and S. Konaka, J. Phys. Chem. A **105**, 6711 (2001).
[31] See supplementary material at http://link.aps.org/supplemental/10.1103/PhysRevE.82.041702 for Torsional energy profiles extracted from the PES of MAB; components and Boltzmann average of the CSTs determined for different MAB conformations; results of the global fitting the 2H NMR data.
[32] C. J. Jameson and H. J. Osten, Annu. Rep. NMR Spectrosc. **17**, 1 (1986).
[33] C. J. Jameson, in *Specialistic Periodic Reports Nuclear Magnetic Resonance*, edited by G. A. Webb (Royal Society of Chemistry, Cambridge, 1994), Vol. 23.
[34] T. Dziembowska, P. E. Hansen, and Z. Rozwadowski, Prog. Nucl. Magn. Reson. Spectrosc. **45**, 1 (2004).
[35] A. Pines, D. J. Ruben, and S. Allison, Phys. Rev. Lett. **33**, 1002 (1974).